Supplement of Atmos. Chem. Phys., 26, 10533–10556, 2026
https://doi.org/10.5194/acp-26-10533-2026-supplement

Atmospheric Chemistry and Physics
Open Access

Supplement of

Surface $PM_{2.5}$ air pollution in 2022 India: emission updates, WRF-Chem model evaluation, and source attribution

Mi Zhou et al.

Correspondence to: Mi Zhou (miz@princeton.edu) and Denise L. Mauzerall (mauzerall@princeton.edu)

S1. Detailed WRF-Chem configuration

S1.1 Selection of months representing each season

The air quality research community widely recognizes four distinct seasons to capture the full range of meteorological and emission variability in India: Winter (Dec–Feb), Pre-Monsoon (Mar–May), Monsoon (Jun–Sep), and Post-Monsoon (Oct–Nov). This four-season structure has been widely adopted in recent literature (Lan et al., 2022; Venkataraman et al., 2024; Zhou et al., 2024; Xie et al., 2024; Kumar et al., 2025). We also note that while some studies may classify September as Post-Monsoon or early June as Pre-Monsoon or December as Post-Monsoon, the four-season structure remains the prevailing framework in India air quality analysis (Conibear et al., 2018; Kota et al., 2018; Reddington et al., 2019; Maheshwarkar et al., 2022; Pai et al., 2022; Sharma et al., 2022; Sharma et al., 2023; Chen et al., 2025).

Our simulation months were selected to represent the distinct pollution and meteorological characteristics of each season:

1) January (Winter): Captures peak anthropogenic emissions and stagnant weather conditions (e.g., low surface wind speed and strong near-surface temperature inversion) (Zhou et al., 2024).
2) April (Pre-Monsoon): Captures dust events, pre-monsoon biomass burning, and higher temperatures.
3) July (Monsoon): Captures monsoon-relevant large precipitations and inflow of ocean air.
4) October (Post-Monsoon): Captures the unique transition period from the monsoon season to winter season, which is heavily influenced by agricultural crop residue burning (Sembhi et al., 2020; Kumari et al., 2021; Lan et al., 2022).

S1.2 Physical Schemes

We configure WRF-Chem with the following physical schemes: the Rapid Radiative Transfer Model for Global Circulation Models (RRTMG) scheme for both shortwave and longwave radiation, which simulates aerosol-radiation interactions (Iacono et al., 2008); the two-moment Morrison microphysics scheme, which simulates aerosol-cloud interactions (Morrison et al., 2005); and the non-local mixing YonSei University (YSU) boundary layer scheme (Hong et al., 2006).

S1.3 The simple secondary organic aerosol (SOA) scheme

The Simple SOA scheme is computationally efficient. In addition, it has also been demonstrated to be robust for regional air quality modeling over Asia. For instance, an earlier study applied this scheme at a 50km resolution and found that, even without modification, it captured observed organic carbon concentrations in polluted urban and suburban environments in China, comparable to more complex, process-based SOA schemes (Miao et al., 2021).

To further support the use of this scheme for India at 27-km resolution, we assessed whether our modeled OA concentrations are within a realistic range. Due to the lack of publicly available ground-based $PM_{2.5}$ speciation data for 2022, we compared our modeled organic aerosol (OA) concentrations with the COALESCE network (Maheshwarkar et al., 2022; Venkataraman et al., 2024), which provides OA observation data from 11 sites across India from 2019. The comparison shows that, on an annual scale, the average OA concentration simulated by WRF-Chem across these 11 sites is 13.0±10.0 μg/m^3, which is consistent with the observed average of 13.5±8.4 μg/m^3. Specifically, for the site near Delhi (Rohtak, Haryana), the model simulates annual OA concentration of 19.3 μg/m^3 compared to the observed 30.0 μg/m^3. While the model underestimates OA by ~30% near Delhi, we consider this performance reasonable given the temporal mismatch (simulating 2022 vs. observing 2019) and the likely decreasing trend in primary OA and SOA precursor emissions under India's National Clean Air Programme (NCAP) launched in 2019.

However, our simulation reports a relatively small annual national population-weighted mean OA concentration (<0.1 μg/m^3) attributed to biogenic emissions from within India. We note that this low estimate likely reflects two factors: (1) The distinct spatial separation between major biogenic sources (e.g., the India-Myanmar border region and Western Ghats) and dense population centers; (2) The inherent limitations of the simple SOA scheme, which has been reported to underestimate the global isoprene-derived SOA budget by ~50% compared to explicit, complex chemistry schemes (Pai et al., 2020). Consequently, our regional simulation provides a conservative lower-bound estimate for biogenic SOA yields in India.

Further evaluation of the simple SOA scheme in India would require contemporaneous observations and the explicit speciation of SOA (distinguishing it from total OA), which is not currently available in the published COALESCE dataset.

S1.4 Mapping aerosol emissions to WRF-Chem variables

Emission inventories provide aerosol emissions of primary organic carbon (POC), black carbon (BC), total primary $PM_{2.5}$, and total primary PM_{10}. While the Emissions Database for Global Atmospheric Research (EDGAR) inventory provides all four types of aerosol emissions, the Community Emissions Data System (CEDS) inventory only includes POC and BC emissions. Total primary $PM_{2.5}$ emissions conceptually comprise primary organic aerosols (POA), BC, and other anthropogenic $PM_{2.5}$ emissions, while total primary PM_{10} emissions include $PM_{2.5}$ and coarse PM emissions. As described in Main Text **Section 2.2.1**, we use all aerosol emissions from EDGAR.

In the selected chemical option (i.e., chem_opt=9, CBMZ_MOSAIC_4BIN_AQ), WRF-Chem reads aerosol emissions as POA, BC, other anthropogenic $PM_{2.5}$, and coarse PM. To map emissions into WRF-Chem variables, we first convert POC to POA emissions using an POC-to-POA ratio of 1.9 for India (Venkataraman et al., 2018). We also enforce the emission constraint that primary $PM_{2.5} \geq BC + POA$. This ensures that the total $PM_{2.5}$ emissions input into WRF-Chem do not exceed those estimated in the merged inventory and prevents negative emissions of other anthropogenic $PM_{2.5}$, which are calculated as $PM_{2.5} - BC - POA$. Coarse PM emissions for WRF-Chem are derived by subtracting $PM_{2.5}$ emissions from PM_{10} emissions.

When distributing aerosol species into the WRF-Chem MOSAIC aerosol bins, we use the default size distribution profiles in the WRF-Chem emission module, which distinguishes between two sources: (1) biomass burning and wildfire sources, and (2) all other sources.

S1.5 Vertical distribution of emissions

Emissions are vertically distributed into WRF-Chem model by sources: (1) agricultural non-burning, residential, and transportation emission are placed at the model's first layer; (2) industrial emissions are distributed within the model's first three layers; (3) power sector emissions are placed within the model's first five layers; (4) natural dust and natural biogenic VOC emissions are placed at the model's first layer; (5) biomass burning emissions are placed vertically using WRF-Chem's online calculated plume rise height.

S2. Additional discussion on WRF-Chem simulation

S2.1 Comparison of source-attributed concentrations before and after scaling

We scale model simulation results (Main Text **Section 2.4**) to ensure mass closure, which forces the sum of all sources' contributions to equal the baseline concentration (with all sector emissions on) within each WRF-Chem grid. In **Table S6**, we present both the scaled contributions and the raw sensitivity estimates (directly derived from baseline minus individual-source-zeroed-out simulations) for each $PM_{2.5}$ component and total $PM_{2.5}$. A comparison between the scaled and raw values indicates that the scaling method results in moderate changes in national annual population-weighted mean concentrations for total $PM_{2.5}$ and its components attributed to a given source. The scaled concentrations differ from the raw calculations by from -5% (i.e., total $PM_{2.5}$ from domestic natural dust) to -20% (i.e., total $PM_{2.5}$ from the domestic agriculture sector). While we acknowledge that the scaling modifies the attributed contribution relative to the raw sensitivity test, we believe this adjusted value is necessary for a mass-balanced budget.

S2.2 AOD underestimation

We interpret the model's AOD underestimation as a diagnostic indication of missing or misrepresented aerosol extinction, rather than as a quantitative source apportionment of the AOD bias. Our baseline simulation substantially underestimates surface coarse PM concentrations compared with CPCB measurements across India, by 37.3 ± 25.7 μg/m^3 ($59 \pm 41\%$; **Fig. S4**). This suggests that missing coarse particulate mass, including fugitive dust from sources not represented in our inventory, such as construction activities and industrial fugitive emissions, may contribute to the AOD low bias. This interpretation is also consistent with previous modelling studies over India that found improved AOD agreement after scaling coarse-particle AOD (David et al., 2018; Singh et al., 2021). However, missing coarse PM alone is unlikely to fully explain the persistent mid-visible AOD underestimation, because visible extinction depends strongly on aerosol size distribution, composition, hygroscopic growth, optical properties and vertical distribution, and fine and accumulation-mode particles generally have higher mass extinction efficiencies than coarse particles.

The AOD bias may therefore also reflect underrepresented fine and accumulation-mode aerosol mass, including primary combustion particles and secondary inorganic and organic aerosol formation. Aerosol water uptake may further contribute to the bias: high local emissions of hydrochloric acid in India can partition into aerosol water and enhance particle growth (Gunthe et al., 2021), but these anthropogenic chloride sources are not represented in the global emission inventories used here. Although this omission has been shown to have a relatively small effect on dry surface $PM_{2.5}$ concentrations (Patel et al., 2024), it can reduce simulated aerosol hygroscopic growth under high relative humidity and thereby contribute to AOD underestimation. Additional uncertainty arises from the treatment of aerosol optical properties in the MOSAIC scheme, including the internal-mixing assumption and the use of four broad size bins, which may not fully resolve the size ranges most efficient for visible-light extinction.

S3. Additional discussion on residential emissions

Residential primary $PM_{2.5}$ emissions in other inventories are significantly lower than those in SMoG (Venkataraman et al., 2018; Venkataraman et al., 2024):

- In 2015: HTAP (2.4 Tg/yr) and EDGAR (1.6 Tg/yr) represent only 73% and 48% of the SMoG $PM_{2.5}$ emission (3.3 Tg/yr), respectively.
- In 2019: While HTAP and EDGAR remain relatively flat (2.4 Tg/yr and 1.6 Tg/yr), SMoG reports a substantial increase to 5.4 Tg/yr. Consequently, HTAP and EDGAR represent only 44% and 30% of the SMoG 2019 $PM_{2.5}$ emission, respectively.
- Current Study: Our updated 2022 residential $PM_{2.5}$ estimate (1.1 Tg/yr) is ~21% of the SMoG 2019 value.

The SMoG 2015 inventory calculates residential emissions based on theoretical energy demand (Pandey et al., 2014; Venkataraman et al., 2018). For example, it utilizes survey-based food consumption data and estimated end-use energy requirements (12 MJ/household-day for cooking) and assumes a theoretical water heating demand (e.g., heating daily water usage to 35 °C). This 'useful energy' methodology likely overestimates actual fuel usage in low-income households subject to fuel poverty, who may 'need' that energy theoretically but cannot afford the fuel to generate it. While the SMoG 2019 publication (Venkataraman et al., 2024) incorporated recent work characterizing non-cooking residential activities based on updated survey data (Navinya et al., 2023), it did not explicitly detail methodological updates for cooking emissions, which remain the dominant source.

In contrast, the residential emission inventory adopted in this study utilized a top-down approach based on actual district-level fuel consumption, derived from comprehensive survey data including the National Family Health Surveys (NFHS-3: 2005–06; NFHS-4: 2015–16; NFHS-5: 2019–21), which were projected to 2022 levels using regression analysis. By relying on reported usage rather than theoretical demand, this approach implicitly captures the affordability constraints and actual consumption habits that define the residential sector in India.

Furthermore, both HTAP and EDGAR inventories typically rely on the International Energy Agency (IEA) World Energy Balances to estimate fuel consumption for the residential sector in India (Janssens-Maenhout et al., 2019; Kurokawa and Ohara, 2020; Guizzardi et al., 2025),

Thus, the underlying source data and methodology differ significantly among these datasets: SMoG relies on energy demand modeling (idealized consumption); Global Inventories rely on IEA statistics (international aggregates); and the inventory adopted in our study is grounded in domestic household survey datasets (actual reported consumption).

S4. Emission Uncertainty Analysis

S4.1 Emission Inventory Uncertainties

- **Global Inventories**: We cannot present quantitative uncertainty ranges for sectoral emissions directly adopted from global inventories (CEDS, EDGAR, and FINN), as these datasets do not provide uncertainty estimates for air pollutant emissions in India.
- **Updated Coal-fired Power Plant Inventory**:
  <u>Activity Data</u>: We directly retrieve plant-level electricity generation and coal consumption reports from the Central Electricity Authority (CEA) of India. We treat this government-reported data as authoritative, and thus focus our uncertainty quantification on emission factors.
  <u>Emission Factors</u>: we establish region-specific uncontrolled emission factors for both domestic coal and imported coal used in India's power plants (**Table S1**). We average the calculated emission factor for a given region if multiple coal composition datasets are found, and present one standard deviation from these calculated values as the uncertainty bounds.
  <u>Total Emissions</u>: We estimate annual total emissions from coal-fired power generation across India in 2022 to be 6.2±1.5 Tg for SO_2, 4.6±0.3 Tg for NO_x, and 0.8±0.1 Tg for primary $PM_{2.5}$, with the range reflecting uncertainties in emission factors without mitigation as reflected in the literature.
- **Updated Residential Emission Inventory**: The residential inventory developed in an earlier study (Velamuri et al., 2024) explicitly conducted an uncertainty analysis using 10,000 Monte-Carlo simulations by sampling emission factors and activity data based on assumed probability distributions for activity levels and emission factors, then extracting 95% confidence bounds from the simulated distribution of total $PM_{2.5}$ emissions. The earlier study assumed the following uncertainties for the residential sector:
  - <u>Activity Data:</u> population (±2.5%), fuel penetration ratios (±5%), and fuel consumption statistics (±5%). Source data is census data and national family health survey reports.
  - <u>Emission Factors:</u> ±25%. Source data is from The Energy and Resources Institute (TERI)'s emission inventory development report (The Energy and Resources Institute, 2021).
  - <u>Total Emissions</u>: ±50% for $PM_{2.5}$.

S4.2 Impact of emission uncertainties on annual source attribution results

We perform a simplified uncertainty propagation analysis for the power and residential sectors to quantify uncertainties associated with their emissions. We approximate uncertainties in the annual national population-weighted mean $PM_{2.5}$ concentration, assuming a near-linear relationship between annual sectoral total emissions and concentration at national level. While we acknowledge limitations of this approach as it does not fully capture non-linearities in secondary chemistry or aerosol-meteorology feedbacks, it serves as a reasonable first-order approximation for the rough estimation. We applied the uncertainty percentages from our emission inventories (as detailed above) to each attributed $PM_{2.5}$ component for these sectors. We then sum the □□□□□□ent-level uncertainties to derive the total uncertainty for the sector's contribution. These estimated uncertainty ranges are presented in **Table S7**.

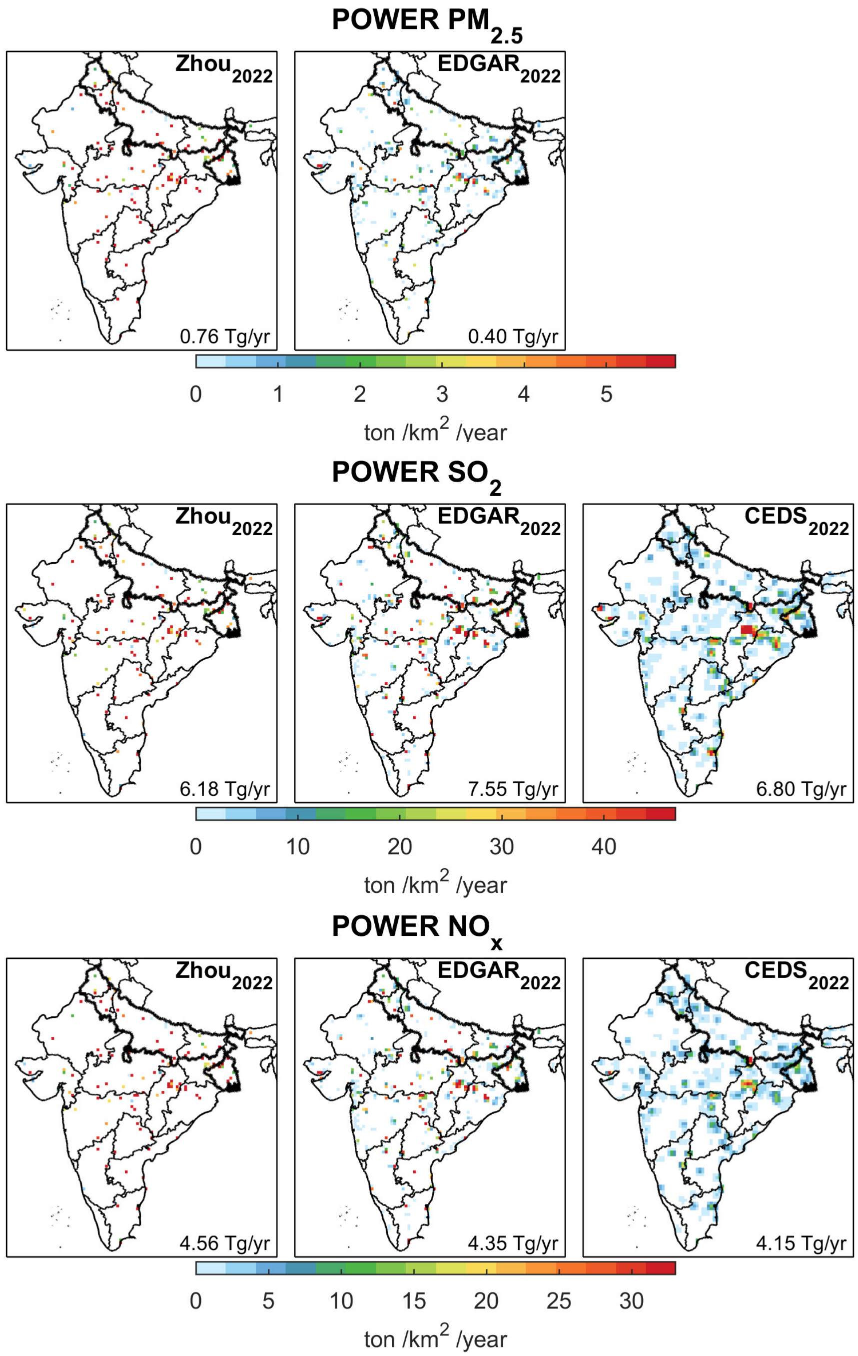

Figure S1. Spatial distribution of 2022 annual power plant emissions of $PM_{2.5}$, SO_2, and NO_x from the inventory developed in this study (Zhou), CEDS, and EDGAR. Our new inventory provides point-source emissions, whereas EDGAR and CEDS report gridded emissions at 0.1° and 0.5° resolution, respectively. For comparison, all inventories are interpolated to the 27 km WRF-Chem model grid. CEDS does not provide primary $PM_{2.5}$ emissions. Numbers inset in each panel indicate annual power plant total emissions across India, and the thick black line denotes the boundary of the Indo-Gangetic Plain (IGP).

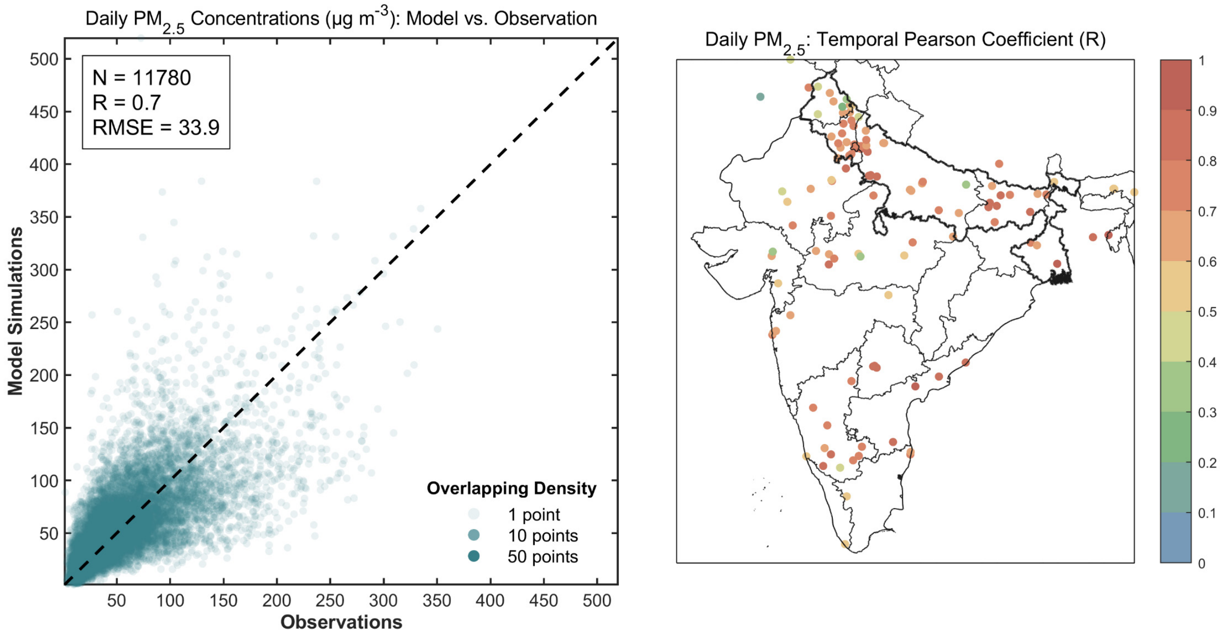

Figure S2. Daily grid-cell-level model evaluation of surface $PM_{2.5}$ concentrations (μg/m^3) for 2022. (a) Density scatter plot of daily modeled versus observed $PM_{2.5}$ for all valid grid-day pairs (N = 11,780), with the dashed line indicating the 1:1 reference. (b) Map of grid-level temporal Pearson correlation coefficients (R) for daily $PM_{2.5}$, where each dot is colored by R value. Thick black lines represent the boundary of the Indo-Gangetic Plain (IGP). Lower temporal R in northwest India likely stem from model bias in simulating natural dust emissions.

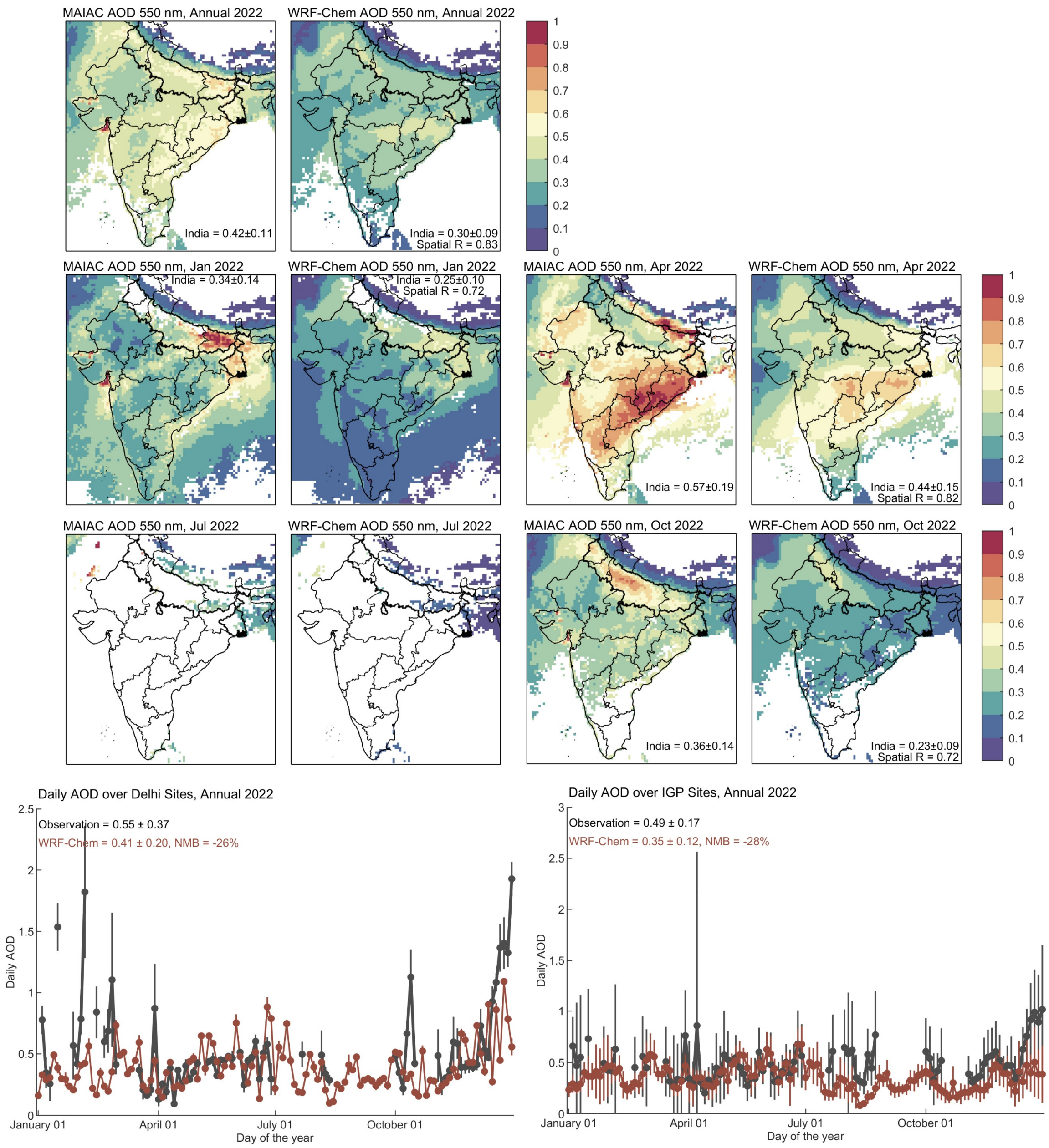

Figure S3. Comparison of WRF-Chem AOD against satellite-derived AOD at 550 nm in 2022. Daily WRF-Chem AOD is derived using mean AOD during 10:00 to 14:00 local time when same day MAIAC AOD is available. In map plots, annual and monthly comparison results are shown for grids with at least 50% valid co-sampled data. Inset numbers in each map plot show the mean ± one standard deviation across India expect for July when there are very few available values. We calculate the Pearson correlation coefficient (Spatial R) between the observed AOD at 550 nm and simulated AOD at 550 nm across India expect for July. The thick black line denotes the boundary of the Indo-Gangetic Plain (IGP) in each map plot. In timeseries plots, we sample MAIAC and WRF-Chem AOD at grids with available $PM_{2.5}$ measurements in each region, and present daily AOD data if at least 50% of the grids (with available $PM_{2.5}$ measurements) in that region have valid AOD data.

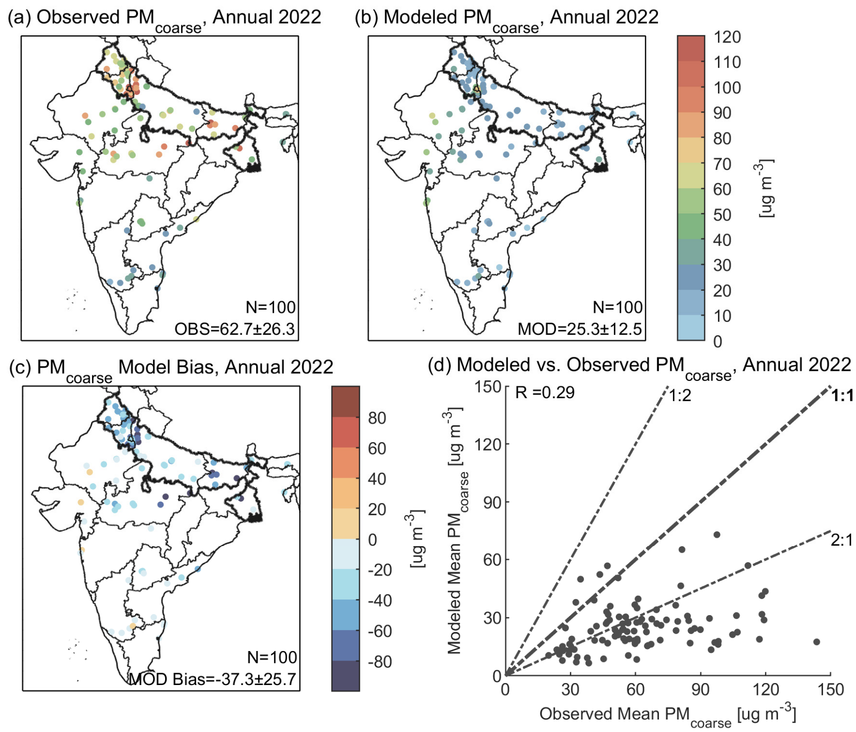

Figure S4. Comparison of observed and modeled surface PM$_{coarse}$ concentrations in 2022 in the baseline simulation. Measurement stations with at least 80% valid hourly data during the four-month period (January, April, July, and October) are selected. Multiple measurements within a single WRF-Chem grid cell are averaged before comparison with WRF-Chem. Annual value is estimated by averaging PM$_{2.5}$ concentrations during the four-month period. In map plots, N denotes the number of grid cells used for evaluation, and the other numbers represent the mean ± one standard deviation across all grid cells. The thick black line denotes the boundary of the Indo-Gangetic Plain (IGP). In the scatter plot, R is the Pearson correlation coefficient between observed and modeled annual mean concentrations across all grid cells.

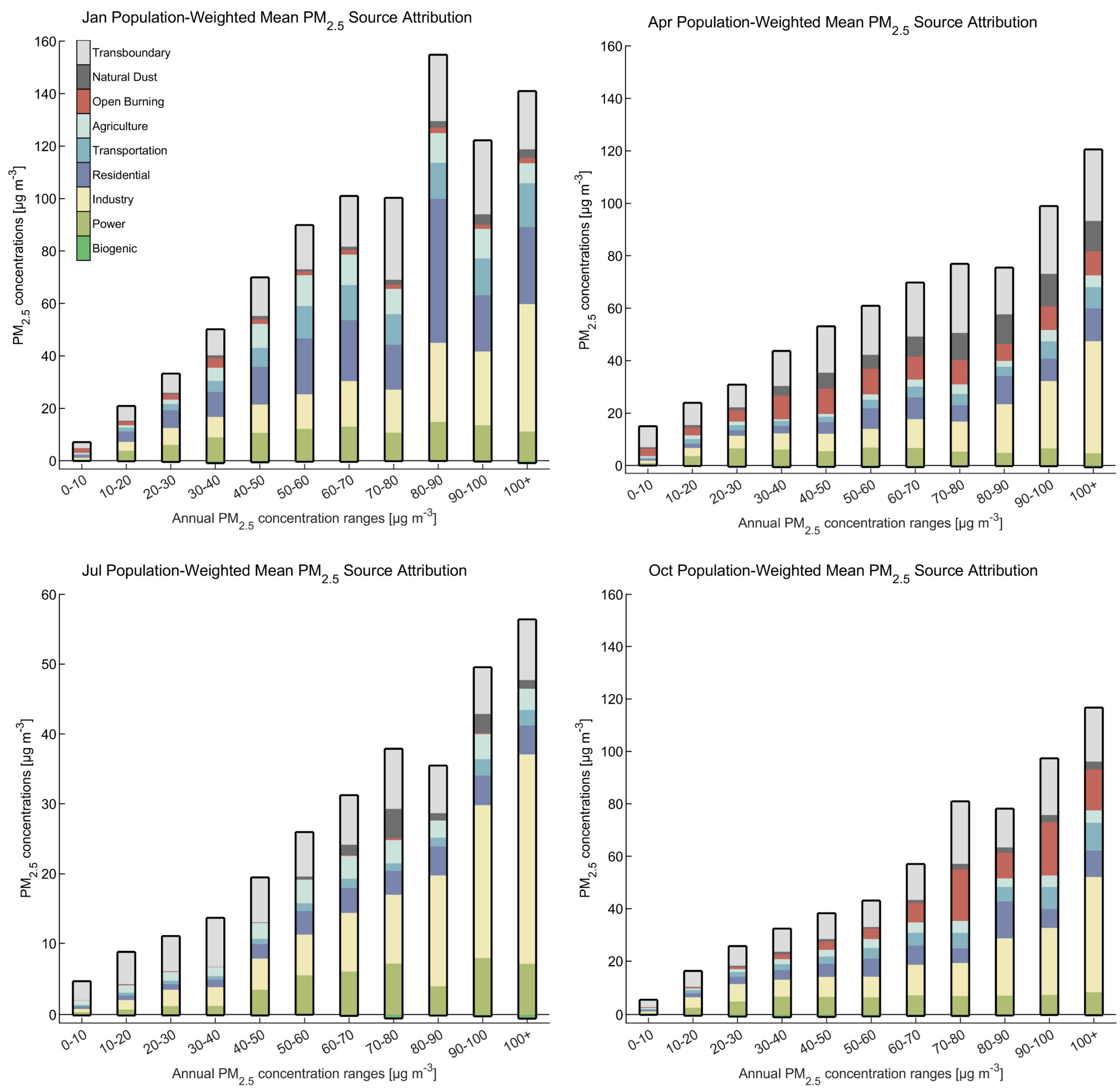

Figure S5. Monthly $PM_{2.5}$ source attribution grouped by annual mean $PM_{2.5}$ concentrations. WRF-Chem grids are aggregated by ranges of annual mean $PM_{2.5}$ concentrations, with colored bars indicating source attribution. See Main Text Figure 5c for the annual version of this figure.

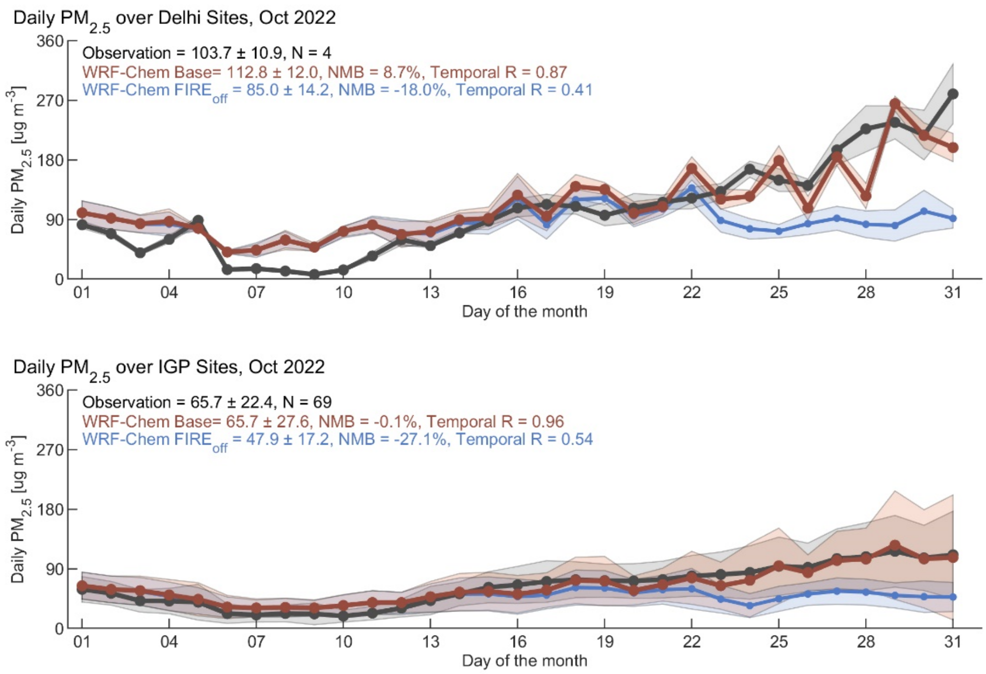

Figure S6. Comparison of observed and modeled (with and without fire emissions) surface $PM_{2.5}$ concentrations in October 2022. Measurement stations with at least 80% valid hourly data are selected. Multiple measurements within a single WRF-Chem grid cell are averaged before comparison with WRF-Chem. N denotes the number of grid cells used for evaluation. Colored lines and dots represent daily and regional mean $PM_{2.5}$ concentrations across available grid cells, with shaded areas indicating one standard deviation across daily mean $PM_{2.5}$ concentrations across those cells. Temporal R is the Pearson correlation coefficient between the red (or blue) and black lines in each panel. NMB is normalized mean bias.

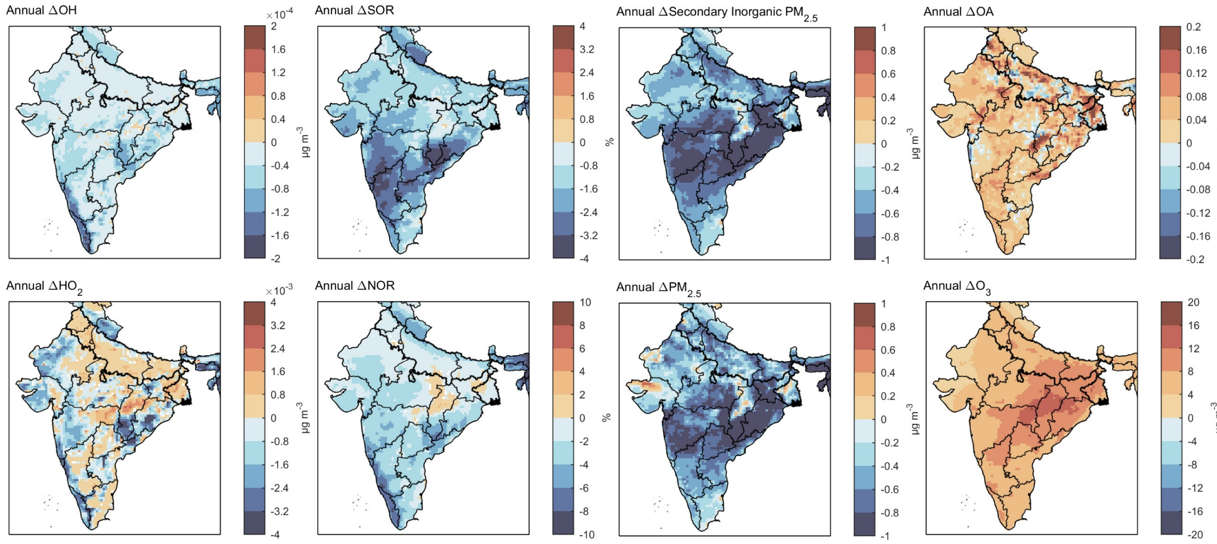

Figure S7. Impact of including Indian BVOC emissions (via turning on the MEGAN module within India) on atmospheric chemistry. All panels are calculated as baseline simulation minus $BVOC_{off}$ simulation. Annual results are calculated as the average of January, April, July, and October simulations. Sulfur Oxidation Ratio (SOR) and Nitrogen Oxidation Ratio (NOR) are calculated as $(SO_4^{2-} + H_2SO_4)/(SO_4^{2-} + H_2SO_4 + SO_2)$ and $(NO_3^- + HNO_3)/(NO_3^- + HNO_3 + NO_2)$, respectively. The thick black line denotes the boundary of the Indo-Gangetic Plain (IGP).

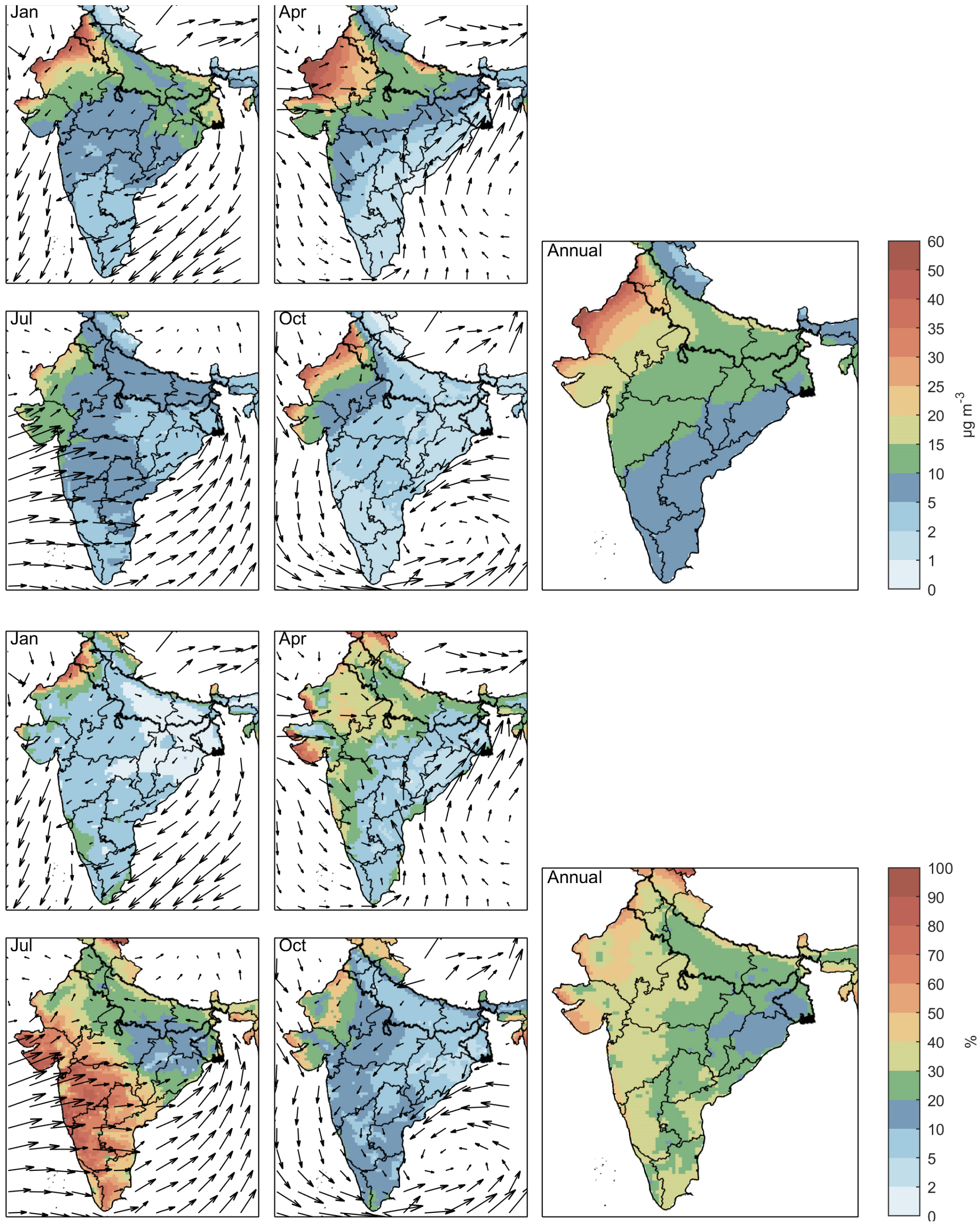

Figure S8. Absolute (upper panels) and percentage (lower panels) contribution of transboundary sources to monthly and annual $PM_{2.5}$ concentrations in 2022. Monthly mean 10-meter wind vectors are also shown to indicate near-surface transport of $PM_{2.5}$ and its precursors. The thick black line denotes the boundary of the Indo-Gangetic Plain (IGP).

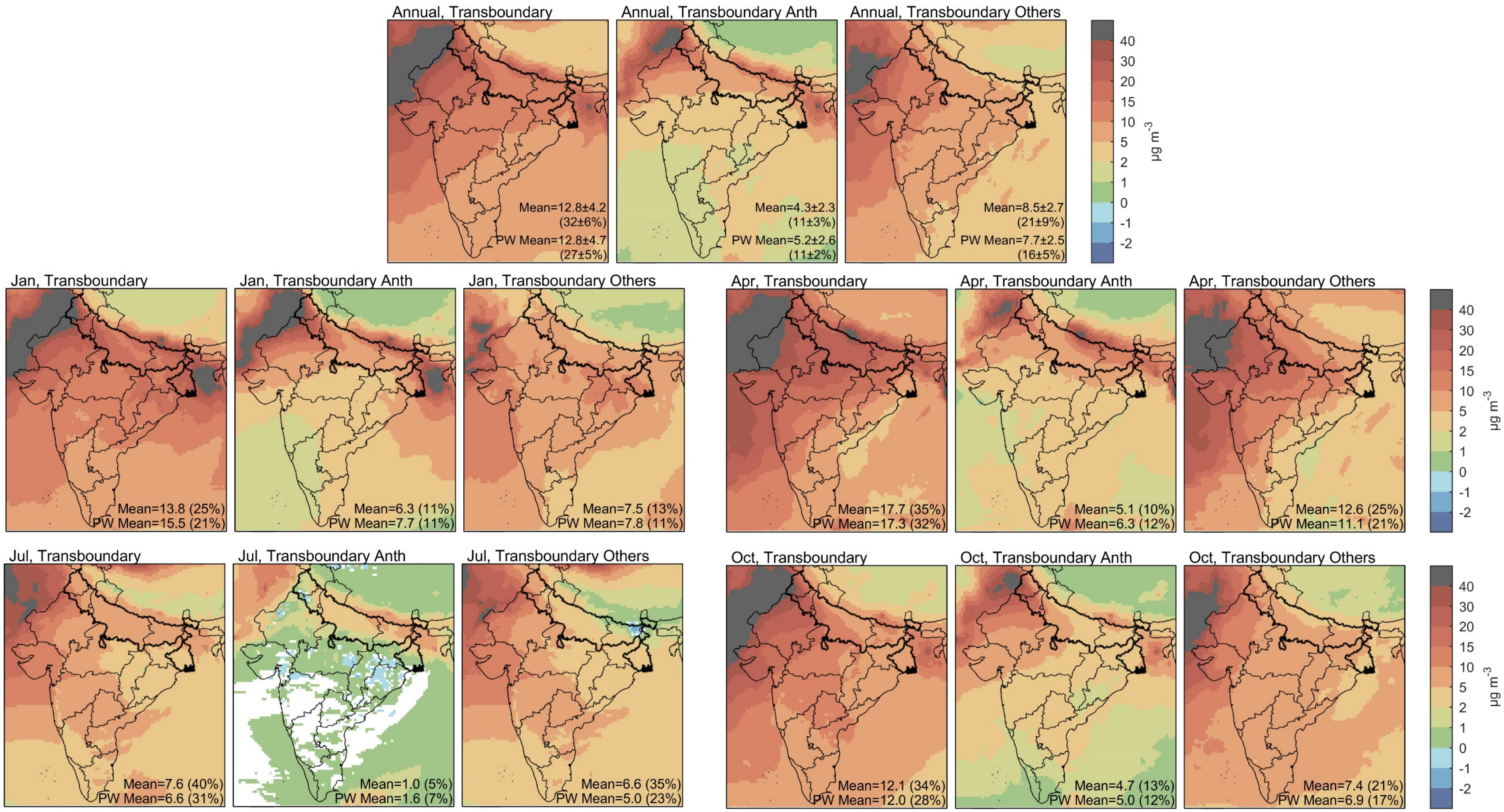

Figure S9. Contributions of transboundary sources to monthly and annual $PM_{2.5}$ concentrations in 2022. Panels are in five groups: Annual, January, April, July, and October. Within these groups the *Left panels*: Total transboundary sources, including both emissions originating outside India but within the WRF-Chem domain (anthropogenic and natural) and long-range transport from regions beyond the domain (from WRF-Chem boundary conditions). *Middle panels*: Transboundary anthropogenic sources, representing anthropogenic emissions specifically emitted outside India but within the modeling domain. *Right panels*: Other transboundary sources, representing the sum of transboundary natural emissions (dust and biogenic) and long-range transport from lateral boundary conditions. The thick black line denotes the boundary of the Indo-Gangetic Plain (IGP).

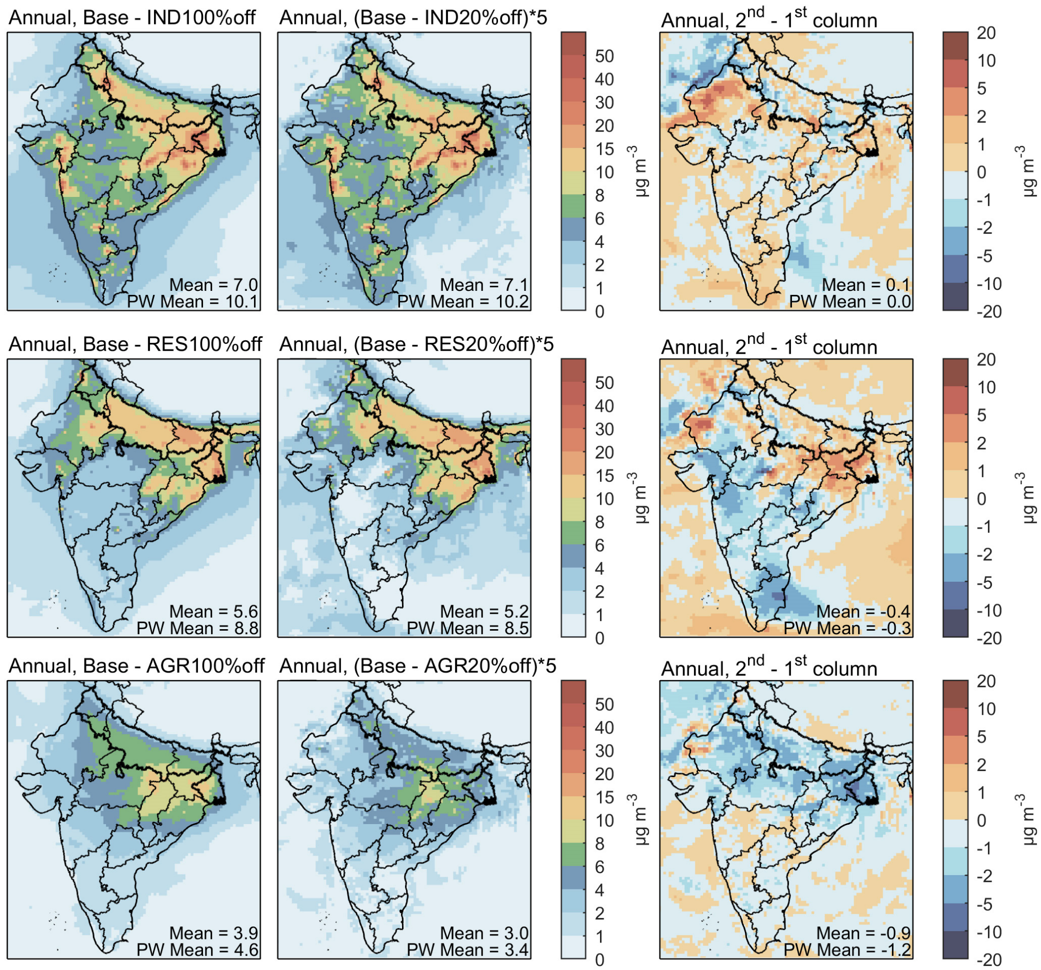

Figure S10. Comparison of $PM_{2.5}$ concentration changes between a 100% emission reduction and a fivefold scaling of 20% reductions. We show results for three sectors: industry (IND), residential (RES), and agriculture (AGR). The thick black line denotes the boundary of the Indo-Gangetic Plain (IGP). Unlike results presented in Main text figures, we **do not** scale concentrations in this figure using **Equation 7**.

Table S1. Uncontrolled emission factors for coal and lignite from various regions used in India's power sector

Source Region	Fuel Classification	CO_2 (g/kg fuel)	SO_2 (g/kg fuel)	NO_x as NO_2 (g/kg fuel)	$PM_{2.5}$ (g/kg fuel)
Assam	Domestic Coal	2329.0±232.9	10.8±1.1	6.0±0.6	1.8±0.2
Chhattisgarh		1204.7±272.7	6.6±0.1		11.4±1.3
Jharkhand		1493.7±408.3	6.8±2.1		9.7±2.2
Madhya Pradesh		1517.0±237.6	6.6±1.2		7.9±3.6
Maharashtra		1501.3±93.0	10.9±7.3		8.1±2.7
Odisha		1062.8±184.3	5.6±1.5		12.7±1.3
Telangana		1396.7±139.7	6.4±0.6		12.2±1.2
Uttar Pradesh		1294.4±129.4	9.2±0.9		10.6±1.1
West Bengal		1810.3±245.9	6.3±1.8		8.5±3.2
Australia	Imported Coal	1913.4±577.2	10.7±7.0		4.5±3.8
Indonesia		1913.4±577.2	10.7±7.0		4.5±3.8
South Africa		2307.2±230.7	8.3±0.8		3.9±0.4
Gujarat, Rajasthan, and Tamil Nadu	Lignite	1250.8±125.1	5.2±0.5	4.0±0.4	1.1±0.1

Source Data: (Kalenga et al., 2011; Mittal et al., 2012; Yunus et al., 2014; Cheepurupalli et al., 2015; Gogoi, 2018; The Singareni Collieries Company Limited, 2018; Dwivedi et al., 2022; U.S. Environmental Protection Agency, 1998)

Table S2. Contribution of Indian sectoral emissions to national total anthropogenic emissions for air pollutants and variation among emission inventories during 2015 to 2022 (average±standard deviation) *

	NO_x	SO_2	$PM_{2.5}$	BC	OC	CO	PM_{coarse}‡	NH_3
Agriculture†	5±0%	0±0%	1±0%	0±0%	0±0%	0±0%	3±0%	85±0%
Industry	19±1%	32±2%	41±5%	38±3%	30±3%	30±1%	37±5%	9±1%
Transportation	29±1%	1±0%	5±1%	13±4%	2±1%	10±1%	1±0%	0±0%
Power	39±0%	61±2%	11±1%	4±1%	4±1%	4±1%	13±9%	1±0%
Residential	8±0%	6±0%	42±2%	45±1%	64±3%	57±1%	46±14%	5±0%

*Results in this table are derived from three global emission inventories: CEDS version 2024-07-08, EDGAR version 8.1, and Hemispheric Transport of Air Pollution (HTAP) version 3.1. Please see Methods for details of how each emission inventory is utilized.

†This excludes agricultural waste burning.

‡PM_{coarse} emissions are estimated by subtracting $PM_{2.5}$ emissions from PM_{10} emissions.

Table S3. Summary of India's power sector emission inventories from this study and previous studies

Inventory	Year of Inventory	Total Coal-based Capacity (GW)	Total Coal-based Generation (TWh/year)	Total Emissions (Tg/year)			Emission Factors (g/kWh)		
				$PM_{2.5}$	SO_2	NO_x (as NO_2)	$PM_{2.5}$	SO_2	NO_x (as NO_2)
This Study*	2022	210.6†	1121.7	0.76	6.18	4.56	0.68	5.51	4.07
(Velamuri et al., 2024)*	2022	210.0	1160.4	0.31	4.70	3.48‡	0.27	4.05	3.00‡
(Singh et al., 2024)*	2019	175.0	948.6	0.58	6.52	4.85	0.61	6.88	5.11
(Cropper et al., 2021)*	2018	208.0	1093.2	0.57	4.86	4.57‡	0.52	4.45	4.18‡
(Guttikunda et al., 2014)*	2010-2011	120.7	689.0	0.58	2.1	2.99‡	0.84	3.05	4.34‡
EDGAR (v8.1) (Crippa et al., 2018)¶	2022	-	-	0.40	7.55	4.35	-	-	-
CEDS (v2024-07-08) (Hoesly et al., 2018)¶	2022	-	-	-	6.80	4.15	-	-	-
HTAP (v3.1) (Guizzardi et al., 2025)¶	2020	-	-	0.66	7.26	2.99	-	-	-
(Venkataraman et al., 2024)¶	2019	-	-	1.70	5.11	2.47	-	-	-
(Venkataraman et al., 2018)¶	2015	-	-	1.07	3.70	2.26	-	-	-

*Inventories only include coal-fired power plants.

¶Inventories include coal, gas, and oil-fired power plants, with coal plants dominating total emissions.

†This value matches the total generation capacity of coal and lignite documented by the Central Electricity Authority (CEA) of India in July 2022.

‡These inventories provide NO_x emissions without specifying the partition between NO and NO_2. We assume a composition of 95% NO and 5% NO_2 for the NO_x emissions reported in these inventories and convert them to NO_2 emissions

Table S4. Summary of model performance of annual $PM_{2.5}$ simulation against surface measurements in each state

	WRF-Chem Mean (μg/m³)	**Observation Mean (μg/m³)**	**Mean Bias* (μg/m³)**	**Normalized Mean Bias¶ (%)**	**Temporal Correlation†**	**Number of model grids**
Andhra Pradesh	30.3±4.7	30.8±5.0	-0.4±5.4	0.3±18.9	0.90	4
Assam	35.80	48.20	-12.50	-25.5	0.54	2
Bihar	55.4±7.9	77.1±11.5	-21.7±11.2	-26.8±15.3	0.89	10
Chandigarh	44.20	47.70	-3.50	-7.3	0.65	1
Delhi	100.2±11.7	99.6±8.0	0.6±16.9	1.6±16.5	0.81	4
Gujarat	66.50	47.50	19.00	50.9	0.54	3
Haryana	63.6±14.6	73.6±12.6	-10.1±10.9	-13.4±16.9	0.80	14
Karnataka	26.9±7.8	25.7±4.6	1.2±6.2	5.1±23.0	0.88	11
Kerala	20.60	17.90	2.70	14.8	0.60	1
Maharashtra	54.3±11.0	40.2±5.7	14.1±6.1	34.1±14.0	0.74	5
Madhya Pradesh	48.5±10.3	50.5±13.3	-2.0±6.9	-1.8±14.0	0.88	10
Nagaland	25.10	27.00	-2.00	-7.2	0.56	1
Punjab	58.3±12.9	48.9±9.0	9.4±17.8	24.4±42.2	0.77	7
Rajasthan	58.7±7.8	51.6±7.3	7.1±12.0	17.0±29.4	0.80	8
Tamil Nadu	24.8	24.2	0.6	5.1	0.79	3
Telangana	44.7	38.9	5.8	14.7	0.88	3
Tripura	45.8	46.5	-0.7	-1.5	0.93	1
Uttar Pradesh	65.5±13.2	62.5±19.3	3.0±19.9	12.5±31.2	0.87	19
West Bengal	76.6±27.3	46.6±9.9	30.0±20.3	60.6±46.3	0.86	4
Foreign	69.0±30.6	75.1±31.4	-6.2±5.5	-8.2±6.1	0.86	5

*Calculated as WRF-Chem Mean minus Observation Mean; ¶Calculated as Mean Bias divided by Observation Mean;

†We first average results for all model grid within a given region, and then estimate the temporal Pearson correlation coefficient between observed and simulated daily $PM_{2.5}$, consistent with Main Text **Figure 3 e** and **g**.

Table S5. Source contribution to 2022 annual population-weighted mean $PM_{2.5}$ nationwide and in each state

(dominant domestic source is highlighted in red)

	Domestic Sources (see the note after this table for full names of each source)								**Transboundary Sources**
	POW	**IND**	**RES**	**TRA**	**AGR**	**FIRE**	**DST**	**BOVC**	
National	6.1 (13%)	8.6 (18%)	7.3 (15%)	3.8 (8%)	3.7 (8%)	3.6 (8%)	1.9 (4%)	-0.5 (-1%)	12.8 (27%)
Andhra Pradesh	5.9 (21%)	6.7 (24%)	3.5 (12%)	1.4 (5%)	1.6 (6%)	1.4 (5%)	0.5 (2%)	-0.5 (-2%)	7.6 (27%)
Arunachal Pradesh	0.9 (6%)	1.7 (12%)	2.1 (15%)	0.5 (3%)	0.6 (4%)	3.6 (25%)	0.2 (1%)	-0.2 (-1%)	4.9 (34%)
Assam	1.9 (7%)	3.1 (11%)	7.9 (28%)	1.2 (4%)	1.3 (4%)	6.0 (21%)	0.3 (1%)	-0.7 (-2%)	7.7 (27%)
Bihar	7.0 (13%)	7.9 (14%)	12.5 (23%)	5.5 (10%)	4.8 (9%)	3.9 (7%)	0.5 (1%)	-0.4 (-1%)	13.7 (25%)
Chhattisgarh	13.5 (24%)	11.4 (20%)	7.0 (12%)	2.4 (4%)	6.0 (11%)	5.6 (10%)	1.1 (2%)	-0.4 (-1%)	10.3 (18%)
Delhi	7.8 (8%)	33.9 (33%)	12.9 (12%)	11.6 (11%)	5.9 (6%)	8.5 (8%)	2.1 (2%)	-0.4 (-0%)	21.0 (20%)
Goa	3.3 (13%)	5.4 (21%)	2.0 (8%)	1.5 (6%)	0.8 (3%)	2.1 (8%)	0.9 (3%)	-0.3 (-1%)	10.7 (41%)
Gujarat	4.1 (7%)	14.2 (25%)	6.2 (11%)	3.1 (6%)	2.3 (4%)	1.7 (3%)	7.2 (13%)	-0.3 (-1%)	17.9 (32%)
Haryana	6.1 (9%)	10.8 (16%)	6.8 (10%)	6.2 (9%)	5.0 (8%)	9.3 (14%)	2.5 (4%)	-0.4 (-1%)	20.4 (31%)
Himachal Pradesh	1.7 (7%)	3.4 (15%)	3.2 (14%)	1.3 (6%)	1.8 (8%)	1.9 (8%)	0.7 (3%)	-0.4 (-2%)	8.8 (39%)
Jammu and Kashmir	1.0 (4%)	1.8 (7%)	4.2 (18%)	1.2 (5%)	1.5 (6%)	0.4 (2%)	0.7 (3%)	-0.3 (-1%)	13.2 (56%)
Jharkhand	10.6 (18%)	13.9 (24%)	7.6 (13%)	4.3 (7%)	6.7 (11%)	4.3 (7%)	0.6 (1%)	-0.5 (-1%)	11.5 (19%)
Karnataka	4.9 (17%)	8.0 (28%)	2.1 (7%)	2.2 (8%)	1.5 (5%)	2.3 (8%)	0.8 (3%)	-0.5 (-2%)	7.9 (27%)
Kerala	3.2 (13%)	6.0 (25%)	3.5 (14%)	2.6 (11%)	0.9 (4%)	1.1 (5%)	0.4 (2%)	-0.4 (-1%)	6.9 (28%)
Ladakh	0.2 (2%)	0.3 (2%)	0.6 (5%)	0.4 (4%)	0.9 (8%)	0.1 (1%)	0.2 (2%)	-0.0 (-0%)	9.1 (77%)
Madhya Pradesh	7.5 (17%)	5.9 (13%)	3.6 (8%)	3.1 (7%)	4.6 (10%)	4.7 (10%)	2.8 (6%)	-0.4 (-1%)	13.5 (30%)
Maharashtra	6.4 (16%)	9.3 (23%)	2.9 (7%)	2.5 (6%)	2.4 (6%)	3.7 (9%)	1.8 (5%)	-0.7 (-2%)	12.0 (30%)
Manipur	2.2 (8%)	3.7 (13%)	3.1 (11%)	0.8 (3%)	1.6 (6%)	7.2 (26%)	0.3 (1%)	-0.8 (-3%)	9.9 (35%)

Meghalaya	2.3 (9%)	3.5 (13%)	4.6 (17%)	1.5 (6%)	1.6 (6%)	4.8 (18%)	0.3 (1%)	-0.9 (-3%)	9.2 (34%)
Mizoram	2.2 (9%)	2.3 (9%)	2.0 (8%)	0.6 (2%)	1.3 (5%)	4.0 (16%)	0.3 (1%)	-0.6 (-3%)	12.9 (52%)
Nagaland	1.8 (6%)	3.0 (10%)	4.6 (16%)	1.1 (4%)	1.4 (5%)	10.1 (34%)	0.3 (1%)	-0.7 (-2%)	7.7 (26%)
Odisha	8.8 (19%)	10.0 (22%)	8.2 (18%)	2.5 (5%)	4.9 (11%)	3.6 (8%)	0.5 (1%)	-0.8 (-2%)	8.3 (18%)
Punjab	3.4 (6%)	7.1 (12%)	6.2 (10%)	4.8 (8%)	3.6 (6%)	10.4 (17%)	1.5 (2%)	-0.4 (-1%)	23.5 (39%)
Rajasthan	4.4 (7%)	5.1 (8%)	7.5 (12%)	4.6 (8%)	4.1 (7%)	2.2 (4%)	10.3 (17%)	-0.4 (-1%)	22.2 (37%)
Sikkim	1.4 (8%)	2.1 (12%)	3.0 (17%)	1.2 (7%)	1.2 (7%)	1.3 (8%)	0.3 (1%)	-0.4 (-3%)	7.2 (42%)
Tamil Nadu	4.6 (21%)	5.2 (24%)	1.9 (9%)	1.5 (7%)	1.1 (5%)	0.9 (4%)	0.4 (2%)	-0.3 (-1%)	6.6 (30%)
Telangana	7.5 (21%)	7.7 (21%)	4.7 (13%)	1.8 (5%)	2.2 (6%)	2.5 (7%)	1.1 (3%)	-0.7 (-2%)	9.1 (25%)
Tripura	2.2 (6%)	2.3 (7%)	9.0 (25%)	1.9 (5%)	1.9 (5%)	3.7 (11%)	0.1 (0%)	-1.1 (-3%)	15.4 (43%)
Uttar Pradesh	6.5 (11%)	9.4 (16%)	10.2 (18%)	6.3 (11%)	5.2 (9%)	4.7 (8%)	1.0 (2%)	-0.4 (-1%)	14.7 (26%)
Uttarakhand	2.1 (7%)	3.4 (12%)	6.0 (21%)	1.8 (6%)	1.7 (6%)	5.1 (17%)	0.6 (2%)	-0.5 (-2%)	8.9 (31%)
West Bengal	7.8 (14%)	11.2 (20%)	15.3 (27%)	4.5 (8%)	5.0 (9%)	2.2 (4%)	0.3 (1%)	-0.3 (-1%)	10.9 (19%)

Abbreviations and their corresponding full names: POW=Power, IND=Industry, RES=Residential, TRA=Transportation, AGR=Agriculture, FIRE= Smoke from Open Burning, DST=Natural Dust, BVOC=Biogenic.

Table S6. Source contribution to 2022 national annual population-weighted mean $PM_{2.5}$ component concentrations

	Domestic Sources*								Transboundary Sources
	POW	**IND**	**RES**	**TRA**	**AGR**	**FIRE**	**DST**	**BVOC**	
Organic	0.4 (0.4)**	2.4 (2.9)	6.6 (7.9)	0.7 (0.8)	0.1 (0.1)	1.3 (1.5)	0.1 (0.1)	<0.1 (<0.1)	2.9 (3.4)
BC	<0.1 (<0.1)	0.9 (1.1)	0.6 (0.7)	0.2 (0.2)	<0.1 (<0.1)	0.2 (0.2)	<0.1 (<0.1)	<0.1 (<0.1)	0.3 (0.3)
Dust	0.9 (1.0)	1.9 (2.2)	0.1 (0.2)	0.5 (0.6)	0.1 (0.1)	1.3 (1.5)	1.8 (2.0)	<0.1 (<0.1)	4.6 (5.3)
Sulfate	2.3 (2.7)	1.5 (1.7)	<0.1 (<0.1)	0.3 (0.3)	0.2 (0.2)	0.1 (0.1)	<0.1 (<0.1)	-0.2 (-0.3)	1.7 (2.0)
Nitrate	1.4 (1.6)	1.1 (1.3)	<0.1 (<0.1)	1.6 (2.0)	2.4 (3.0)	0.5 (0.6)	<0.1 (<0.1)	-0.1 (-0.1)	1.9 (2.2)
Ammonium	1.2 (1.5)	0.8 (1.0)	<0.1 (<0.1)	0.6 (0.7)	0.8 (1.1)	0.2 (0.2)	<0.1 (<0.1)	-0.1 (-0.1)	1.1 (1.3)
Sodium and Chloride	<0.1 (<0.1)	<0.1 (<0.1)	<0.1 (<0.1)	<0.1 (<0.1)	0.1 (0.1)	<0.1 (<0.1)	<0.1 (<0.1)	<0.1 (<0.1)	0.4 (0.4)
Total	6.1 (7.4)	8.6 (10.1)	7.3 (8.8)	3.8 (4.7)	3.7 (4.6)	3.6 (4.1)	1.9 (2.0)	-0.5 (-0.5)	12.8 (14.9)

*Abbreviations and their corresponding full names: POW=Power, IND=Industry, RES=Residential, TRA=Transportation, AGR=Agriculture, FIRE=Smoke from Open Burning, DST=Natural Dust, BVOC=Biogenic.

**Values outside parentheses are scaled contributions calculated using Equation 7, while values inside parentheses represent raw estimates directly derived from (baseline minus individual-source-zeroed-out) model simulations.

Table S7. Uncertainty estimation of 2022 national annual population-weighted mean $PM_{2.5}$ component concentrations for the power and residential sectors

Species	Domestic Sources	
	Power	**Residential**
Organic	0.42±0.05	6.60±3.30
BC	0.01±0.00	0.58±0.29
Dust	0.99±0.12	0.13±0.06
Sulfate	2.80±0.67	-0.01±0.00
Nitrate	0.81±0.05	-0.01±0.00
Ammonium	1.11±0.25	-0.01±0.00
Total $PM_{2.5}$	6.11±1.14	7.28±3.65

Reference:

Cheepurupalli, N. R., Sharma, G. V. S., Singh, C. S., and Rao, E. N. D.: Petrographic Analysis and its Relationship with Calorific Values of Non- Coking Coals, Talcher Coalfield, Orissa, International Journal of Engineering Trends and Technology, 2015.

Chen, Y., van der A, R. J., Ding, J., Eskes, H., Williams, J. E., Theys, N., et al.: SO2 emissions derived from TROPOMI observations over India using a flux-divergence method with variable lifetimes, Atmospheric Chemistry and Physics, 25, 1851-1868, 2025.

Conibear, L., Butt, E. W., Knote, C., Arnold, S. R., and Spracklen, D. V.: Residential energy use emissions dominate health impacts from exposure to ambient particulate matter in India, Nat Commun, 9, 617, 2018.

Crippa, M., Guizzardi, D., Muntean, M., Schaaf, E., Dentener, F., van Aardenne, J. A., et al.: Gridded emissions of air pollutants for the period 1970–2012 within EDGAR v4.3.2, Earth System Science Data, 10, 1987-2013, 2018.

Cropper, M., Cui, R., Guttikunda, S., Hultman, N., Jawahar, P., Park, Y., et al.: The mortality impacts of current and planned coal-fired power plants in India, Proc Natl Acad Sci U S A, 118, 2021.

David, L. M., Ravishankara, A. R., Kodros, J. K., Venkataraman, C., Sadavarte, P., Pierce, J. R., et al.: Aerosol Optical Depth Over India, J Geophys Res Atmos, 123, 3688-3703, 2018.

Dwivedi, A. and Kumar, A.: Investigations of the Ultimate and Proximate Analysis of Coal Samples from the Singrauli Coalfield, India, International Journal of Current Science Research and Review, 2022.

Gogoi, K.: Geochemical Characteristics of Tertiary Coals of Collieries of Makum Coalfield: Implication to Depositional Environment, Journal of Emerging Technologies and Innovative Research, 2018.

Guizzardi, D., Crippa, M., Butler, T., Keating, T., Wu, R., Kamiński, J. W., et al.: The HTAP_v3.1 emission mosaic: merging regional and global monthly emissions (2000–2020) to support air quality modelling and policies, 2025.

Gunthe, S. S., Liu, P., Panda, U., Raj, S. S., Sharma, A., Darbyshire, E., et al.: Enhanced aerosol particle growth sustained by high continental chlorine emission in India, Nature Geoscience, 14, 77-84, 2021.

Guttikunda, S. K. and Jawahar, P.: Atmospheric emissions and pollution from the coal-fired thermal power plants in India, Atmos Environ, 92, 449-460, 2014.

Hoesly, R. M., Smith, S. J., Feng, L., Klimont, Z., Janssens-Maenhout, G., Pitkanen, T., et al.: Historical (1750–2014) anthropogenic emissions of reactive gases and aerosols from the Community Emissions Data System (CEDS), Geosci Model Dev, 11, 369-408, 2018.

Hong, S. Y., Noh, Y., and Dudhia, J.: A new vertical diffusion package with an explicit treatment of entrainment processes, Mon Weather Rev, 134, 2318-2341, 2006.

Iacono, M. J., Delamere, J. S., Mlawer, E. J., Shephard, M. W., Clough, S. A., and Collins, W. D.: Radiative forcing by long-lived greenhouse gases: Calculations with the AER radiative transfer models, Journal of Geophysical Research: Atmospheres, 113, 2008.

Kalenga, P. M., Cukrowska, E., Tutu, H., and Chimuka, L.: Characterization of South African Coal for Metals, Inorganic and Organic Sulfur Compounds, S Afr J Chem-S-Afr T, 64, 254-262, 2011.

Kota, S. H., Guo, H., Myllyvirta, L., Hu, J., Sahu, S. K., Garaga, R., et al.: Year-long simulation of gaseous and particulate air pollutants in India, Atmos Environ, 180, 244-255, 2018.

Kumar, A., Imam, F., Dixit, K., Chaudhary, E., Sharma, S., Singh, N., et al.: Sectoral Contributions to Primary and Secondary PM2.5 in Regional Airsheds of India, ACS Earth and Space Chemistry, 2025.

Kumari, S., Verma, N., Lakhani, A., and Kumari, K. M.: Severe haze events in the Indo-Gangetic Plain during post-monsoon: Synergetic effect of synoptic meteorology and crop residue burning emission, Sci Total Environ, 768, 145479, 2021.

Lan, R., Eastham, S. D., Liu, T., Norford, L. K., and Barrett, S. R. H.: Air quality impacts of crop residue burning in India and mitigation alternatives, Nature Communications, 13, 2022.

Maheshwarkar, P., Ralhan, A., Raman, R. S., Tibrewal, K., Venkataraman, C., Dhandapani, A., et al.: Understanding the Influence of Meteorology and Emission Sources on PM2.5 Mass Concentrations Across India: First Results From the COALESCE Network, J Geophys Res-Atmos, 127, 2022.

Miao, R., Chen, Q., Shrivastava, M., Chen, Y., Zhang, L., Hu, J., et al.: Process-based and observation-constrained SOA simulations in China: the role of semivolatile and intermediate-volatility organic compounds and OH levels, Atmospheric Chemistry and Physics, 21, 16183-16201, 2021.

Mittal, M., Sharma, C., and Singh, R.: Estimates of emissions from coal fired thermal power plants in India, https://www.researchgate.net/publication/267687877_Estimates_of_Emissions_from_Coal_Fired_Thermal_Power_Plants_in_India, 2012.

Morrison, H. and Pinto, J. O.: Mesoscale modeling of springtime Arctic mixed-phase stratiform clouds using a new two-moment bulk microphysics scheme, Journal of the Atmospheric Sciences, 62, 3683-3704, 2005.

Navinya, C., Kapoor, T. S., Anurag, G., Lokhande, P., Sharma, R., Prasad, S. L., et al.: Heating and lighting: understanding overlooked energy-consumption activities in the Indian residential sector, Environ Res Commun, 5, 2023.

Pai, S. J., Heald, C. L., Coe, H., Brooks, J., Shephard, M. W., Dammers, E., et al.: Compositional Constraints are Vital for Atmospheric PM(2.5) Source Attribution over India, ACS Earth Space Chem, 6, 2432-2445, 2022.

Pai, S. J., Heald, C. L., Pierce, J. R., Farina, S. C., Marais, E. A., Jimenez, J. L., et al.: An evaluation of global organic aerosol schemes using airborne observations, Atmospheric Chemistry and Physics, 20, 2637-2665, 2020.

Pandey, A., Sadavarte, P., Rao, A. B., and Venkataraman, C.: Trends in multi-pollutant emissions from a technology-linked inventory for India: II. Residential, agricultural and informal industry sectors, Atmos Environ, 99, 341-352, 2014.

Patel, A., Reddy, M. C., Liu, P., and Gunthe, S. S.: Impact of Continental Cl• -N2O5 Multiphase Heterogeneous Chemistry on Regional Air Chemistry: A GEOS-Chem study over Indian Region, https://essopenarchive.org/doi/full/10.22541/essoar.173482078.82609568, 2024.

Reddington, C. L., Conibear, L., Knote, C., Silver, B. J., Li, Y. J., Chan, C. K., et al.: Exploring the impacts of anthropogenic emission sectors on PM_{2.5} and human health in South and East Asia, Atmospheric Chemistry and Physics, 19, 11887-11910, 2019.

Sembhi, H., Wooster, M., Zhang, T., Sharma, S., Singh, N., Agarwal, S., et al.: Post-monsoon air quality degradation across Northern India: assessing the impact of policy-related shifts in timing and amount of crop residue burnt, Environmental Research Letters, 15, 2020.

Sharma, A., Venkataraman, C., Muduchuru, K., Singh, V., Kesarkar, A., Ghosh, S., et al.: Aerosol radiative feedback enhances particulate pollution over India: A process understanding, Atmos Environ, 298, 2023.

Sharma, D. and Mauzerall, D.: Analysis of Air Quality Data in India between 2015 and 2019, Aerosol and Air Quality Research, 22, 2022.

Singh, K., Peshin, T., Sengupta, S., Thakrar, S. K., Tessum, C. W., Hill, J. D., et al.: Air pollution mortality from India's coal power plants: unit-level estimates for targeted policy, Environmental Research Letters, 19, 2024.

Singh, N., Agarwal, S., Sharma, S., Chatani, S., and Ramanathan, V.: Air Pollution Over India: Causal Factors for the High Pollution with Implications for Mitigation, ACS Earth and Space Chemistry, 2021.

THE SINGARENI COLLIERIES COMPANY LIMITED: The point wise replies for ADS, THE SINGARENI COLLIERIES COMPANY LIMITED, https://environmentclearance.nic.in/writereaddata/Online/EDS/0_0_05_Mar_2019_1952195131AnnexADSreply.pdf, 2018.

U.S. Environmental Protection Agency: Bituminous And Subbituminous Coal Combustion, U.S. Environmental Protection Agency, https://www.epa.gov/sites/default/files/2020-09/documents/1.1_bituminous_and_subbituminous_coal_combustion.pdf, 1998.

Velamuri, V., Nayak, D. K., Sharma, S., Parmar, P. D., Nagar, P. K., Singh, D., et al.: India leads in emission intensity per GDP: Insights from the gridded emission inventory for residential, road transport, and energy sectors, Journal of Environmental Sciences, 2024.

Venkataraman, C., Brauer, M., Tibrewal, K., Sadavarte, P., Ma, Q., Cohen, A., et al.: Source influence on emission pathways and ambient PM2.5 pollution over India (2015-2050), Atmos Chem Phys, 18, 8017-8039, 2018.

Venkataraman, C., Anand, A., Maji, S., Barman, N., Tiwari, D., Muduchuru, K., et al.: Drivers of PM2.5 Episodes and Exceedance in India: A Synthesis From the COALESCE Network, Journal of Geophysical Research: Atmospheres, 129, 2024.

Xie, Y., Zhou, M., Hunt, K. M. R., and Mauzerall, D. L.: Recent PM2.5 air quality improvements in India benefited from meteorological variation, Nat Sustain, 2024.

Yunus, M., Asadullah, M., A. Ghulman, H., Rahman, F., and Irfan, M.: Energy Based Analysis of a Thermal Power Station for Energy Efficiency Improvement, International Journal Of Modern Engineering Research, 2014.

Zhou, M., Xie, Y., Wang, C., Shen, L., and Mauzerall, D. L.: Impacts of current and climate induced changes in atmospheric stagnation on Indian surface PM(2.5) pollution, Nat Commun, 15, 7448, 2024.